




# Fatigue behavior of unidirectional fiber-reinforced pultruded composites with high volume fiber fraction

Omar Alajarmeh<sup>1</sup>  | Allan Manalo<sup>1</sup> | Wahid Ferdous<sup>1</sup> | Ghassan Almasabha<sup>2</sup>  | Ahmad Tarawneh<sup>2</sup>  | Khaled Eayal Awwad<sup>3</sup> | Alexander Safonov<sup>4</sup> | Xuesen Zeng<sup>1</sup> | Peter Schubel<sup>1</sup>

<sup>1</sup>Centre for Future Materials, University of Southern Queensland, Toowoomba, Queensland, Australia

<sup>2</sup>Civil Engineering Department, Faculty of Engineering, The Hashemite University, Zarqa, Jordan

<sup>3</sup>Department of Mechanical Engineering, Tafila Technical University, Tafilah, Jordan

<sup>4</sup>Centre for Design, Manufacturing and Materials, Skolkovo Institute of Science and Technology, Moscow, Russia

## Correspondence

Omar Alajarmeh, Centre for Future Materials, University of Southern Queensland, Toowoomba, Queensland 4350, Australia.  
Email: [omar.alajarmeh@usq.edu.au](mailto:omar.alajarmeh@usq.edu.au)

## Funding information

Advance Queensland Industry Research Fellowship Program, Grant/Award Number: AQIRF128-2021

## Abstract

Pultrusion is a high-volume manufacturing process for fiber-reinforced polymer (FRP) composites ensuring high strength and quality products. However, research studies are very limited on the fatigue behavior of these products, especially with unidirectional fiber alignment. This study investigates the fatigue behavior of the unidirectional pultruded glass FRP (GFRP) composites with high fiber volume fraction ( $V_f = 65\%$ ). Tension–tension fatigue loading was applied with different levels of applied stress, frequency, and gripping condition until failure. Results showed that the high  $V_f$  composites have significantly low fatigue life cycle. Moreover, increasing the frequency showed better fatigue resistance, while the tabs geometry has insignificant effect on the fatigue behavior of the dog-bone shaped specimens. Comparison with available literature showed that GFRP composites with high  $V_f$  have lower fatigue performance than those with low  $V_f$ . A fatigue capacity reduction factor is also proposed for unidirectional GFRP composites as a function of the  $V_f$ .

## KEYWORDS

fatigue, fiber volume fraction, frequency, GFRP, pultrusion, reduction factor, S-N curve, unidirectional fibers

## Highlights

- High  $V_f$  UD GFRP composites were manufactured and tested under fatigue loading.
- Influence of applied stress, frequency, and gripping on the fatigue life of composites were studied.
- Fatigue life of UD GFRP composites with various  $V_f$  was compared and analyzed.
- This study proposes a fatigue reduction factor based on the value of  $V_f$  for design purposes.

This is an open access article under the terms of the [Creative Commons Attribution-NonCommercial](https://creativecommons.org/licenses/by-nc/4.0/) License, which permits use, distribution and reproduction in any medium, provided the original work is properly cited and is not used for commercial purposes.

© 2023 The Authors. *Fatigue & Fracture of Engineering Materials & Structures* published by John Wiley & Sons Ltd.

## 1 | INTRODUCTION

Fiber-reinforced polymer (FRP) composites have been widely utilized in aerospace, automobile, wind blades, and various civil applications.<sup>1</sup> The advantageous characteristics of FRP material can be summarized by their high strength-to-weight ratio, corrosion resistance, neutral electromagnetic interference, and ease of manufacture. Thus, it is essential to investigate the behavior of FRP material under different loading conditions to exploit further their unique advantages and maximize their application in different engineering applications.

Among various loading conditions, fatigue (defined as a degradation in life cycle resistance of the material until complete failure) is considered a crucial design consideration for structural FRP composites due to its sudden failure behavior.<sup>2</sup> FRP composites in civil infrastructure applications will be subjected to repetitive loads, but their fatigue behavior has received limited attention to date.<sup>1</sup> Available studies have investigated the fatigue behavior of the FRP composites manufactured using various techniques such as hand-layup,<sup>3</sup> vacuum bagging<sup>4</sup> and infusion,<sup>5</sup> and resin transfer molding<sup>6</sup> considering various fiber types<sup>7</sup> and fiber alignment/orientation.<sup>8</sup> However, the fiber volume fraction ( $V_f$ ) of these studied composites is less than 60% due to the limitation of the compaction process to achieve high fiber content.

Today, the application of composites is limited by their cost and manufacturing complexity (hand layup, autoclave processes, etc.). On the other side, there is increasing demand due to trend of vehicle electrification, which requires low weight to achieve range targets. Pultrusion therefore enables high-rate production and quite automated process, which may be a break-through in adopting composites more as “off the shelf components.” Moreover, pultrusion can produce FRP composites with  $V_f$  even higher than 60% by pulling the resin-impregnated glass fibers through a heating die obtaining immediate cured composites.<sup>9–11</sup> This allows the pultrusion process to become a cost-effective process in manufacturing FRP composites at commercial scale. It is worth mentioning that increasing the  $V_f$  contributes to increasing the stiffness, which majorly affects the design and the weight of structures.<sup>10,12–14</sup> However, the fatigue behavior of the pultruded FRP composites with high  $V_f$  needs to be investigated.

Very limited studies can be found on the fatigue behavior of unidirectional (UD) FRP composites<sup>4,5,15–18</sup> with a lack of consideration of UD FRP composites with fiber volume fraction ( $V_f$ ) higher than 60%. It was

reported that the composites with high  $V_f$  (more than 60%) are designed in special cases to obtain high tensile properties.<sup>19,20</sup> However, it might contribute to a deterioration in other mechanical properties.<sup>21</sup> Due to the anisotropic nature of the FRP composites, the amount of fiber content plays a major role in defining the failure initiation and progression as the resin-fiber interface changes.<sup>22</sup> Thus, a variety of complex failure mechanisms under fatigue loading can be observed including resin microcracks, delamination, interfacial matrix-fiber shear cracks, fiber rupture, and pullout.<sup>4,5,15–18,22</sup> According to the previous studies, these observations were affected by material constituents (fiber<sup>23</sup> and resin<sup>24</sup> types, fiber content,<sup>16,25</sup> and fiber orientation and structure<sup>5,7</sup>) and testing parameters (the maximum and minimum stress amplitude [stress ratio], applied stress level, and end gripping condition<sup>3,24</sup>). It is worth mentioning that the applied stress and the number of cycles (S-N) curve is considered as the fatigue characteristic of a material which shows the decrease in applied stress with the increase in the number of cycles in an exponential or logarithmic scheme.<sup>26</sup>

Based on material constituents, for instance, Wu et al.<sup>23</sup> stated that carbon unidirectional FRP sheets showed better fatigue life behavior than their glass counterpart due to the difference in the interfacial bond between the matrix and the fiber. Ferdous et al.<sup>24</sup> reported that polyester resin performed better fatigue behavior compared to the vinyl ester resin where the latter showed a more rigid bond to the fibers causing higher self-heating, which led to more stress concentration. Moreover, Mini et al.<sup>25</sup> tested glass woven fabric with a various fiber volume fraction ( $V_f$ ) (34% to 57%) under transverse fatigue loading. They stated that specimens with high  $V_f$  showed satisfactory fatigue life but exhibited earlier failure due to the reduction in the amount of matrix sufficient for bonding the fibers. For the same reason, Brunbauer and Pinter<sup>27</sup> reached to the same conclusion when testing unidirectional glass FRP specimens with  $V_f$  of 30% and 55%. They have reported that increasing the  $V_f$  resulted in changing the failure mode from matrix cracking and matrix-fiber debonding to fiber pullout. Furthermore, Brunbauer et al.<sup>18</sup> tested carbon/epoxy laminates with 0°, 45°, and 90° fiber orientation. They observed a change in the mode of failure from fiber pullout to matrix fracture when the fiber angle changed from 0° to 90°. In addition, the fatigue life was reduced when changing the angle from 0° to 90° as the stress concentrated in the matrix zones. This concludes that there are still few studies in this field, and there is a need to build a bigger database of knowledge. This further highlights the importance of evaluating the fatigue performance of FRP composites.

There are many testing parameters on the other hand that are influencing the fatigue life behavior of FRP composites including the stress amplitude (stress ratio), applied stress level, the frequency, and the end gripping condition.<sup>3,5,8,28</sup> For instance, Ferdous et al.<sup>3</sup> stated that increasing the applied fatigue stress made the mode of failure more progressive, while specimens showed localized failure at low fatigue stress. They have shown that specimens tested at a maximum frequency of 8 Hz did not show a significant increase in their self-heating. Moreover, Korhikoski et al.<sup>5</sup> studied the effect of the specimen shape under fatigue loading. They have confirmed that the dog-bone shape revealed a better representation of the actual fatigue life of composite specimens compared to the rectangular one due to the release of the stress concentration at the contact point between the specimen and the grip. Furthermore, Mohammadi and Fazlali<sup>8</sup> investigated the effect of the stress amplitude (stress ratio) on the fatigue behavior of the FRP composites with different fiber orientations. They showed that the increase in the tension-tension stress ratio from 0 to 0.1 and 0.5 enhanced the fatigue life of FRP composites due to the reduced applied energy at every cycle resulting in more cycles before failure. A similar finding was published by Zhao et al.<sup>29</sup> However, selecting a stress ratio of 0.1 exhibited a more realistic load-carrying scenario in structures as supported by Hashin and Rotem<sup>2</sup> and Toth<sup>30</sup> as the increase in the stress ratio increases significantly the delamination growth rate resulting in nonrealistic fatigue behavior of the FRP composites.<sup>31</sup> These studies showed that there are many important parameters that affect the fatigue life of FRP composites, which require detailed investigations.

Understanding the influence of different material constituents at different test parameters on the fatigue life of FRP composites is important in their optimized manufacturing and effective design. This study, therefore, aims at investigating the fatigue behavior of pultruded UD GFRP composites with high fiber volume fraction ( $V_f$ ) of 65% considering various testing parameters including frequency (4, 6, 8, and 10 Hz) and specimen end conditions (with and without tabs) under various applied stress (40%, 60%, and 80% of the ultimate tensile strength [UTS]). The effect of the  $V_f$  is analyzed and compared with the results from available literature for UD composites with lower  $V_f$ . The results of this study will aid composite manufacturers on optimum fiber content to maximize the performance of their products and for designers in accounting for the long-term fatigue resistance of unidirectional GFRP composites in the design of structural applications subject to repeated loads.

## 2 | MANUFACTURING OF SPECIMENS AND DESIGN OF EXPERIMENT

### 2.1 | Manufacturing of specimens

The tested specimens in this study were manufactured using a pultrusion machine (Pultrex) at the University of Southern Queensland with three tons pull capacity. The manufacturing process was achieved by pulling the impregnated unidirectional 4400tex ECR E-glass fibers (supplied by JUSHI-China) with a filament diameter between 20 and 30  $\mu\text{m}$  in vinyl ester resin (VIAPAL ZUP 4617/50—supplied by Allnex-Australia) through 1 m long heating die with a uniform temperature of 120°C at 500 mm/min. The pultrusion process of a 3.25-mm-thick and 50-mm-wide FRP strip is shown in Figure 1. Differential scanning calorimeter (DSC) test conducted revealed that the produced composites achieved a 99.1% ( $\pm 0.2\%$ ) degree of cure. Glass transition temperature ( $T_g$ ) was measured to be 138°C ( $\pm 2.1^\circ\text{C}$ ) in accordance with ASTM E1269.<sup>32</sup> Burnout test conducted following ASTM D 3171-15<sup>33</sup> showed that the fiber content and fiber volume fraction were 82.4% (standard deviation of 0.13%) and 65.0% (standard deviation of 0.11%), respectively.

### 2.2 | Specimen design and testing parameters

A 3.25-mm-thick pultruded flat plate was used to cut the testing specimens in a dog-bone shape in accordance with ASTM D3479<sup>34</sup> and ASTM D638<sup>35</sup> with overall dimensions shown in Figure 2A. The dog-bone shape was adopted as it was found to accurately represent the fatigue life of the composites.<sup>5</sup> Another set of specimens was prepared to examine the effect of the end condition on the fatigue behavior of the UD composites by providing tabs at the ends of the dog-bone specimens. The tabs were cut from the same pultruded plate and glued using Techniglu (R60 from ATL Composites) (see Figure 2B).

This study investigated the effect of the applied stress levels, that is, 80%, 60%, and 40% (from high to low, respectively) of the UTS of the control specimens. Five specimens were tested under quasi-static loading (1 mm/min) until failure as control samples in accordance with ASTM D638<sup>35</sup> and ASTM D3039.<sup>36</sup> Each level of strength was tested considering various frequency values including 4, 6, 8, and 10 Hz to find the influence of the loading frequency on the fatigue behavior of the UD glass FRP specimens. This range of frequency was

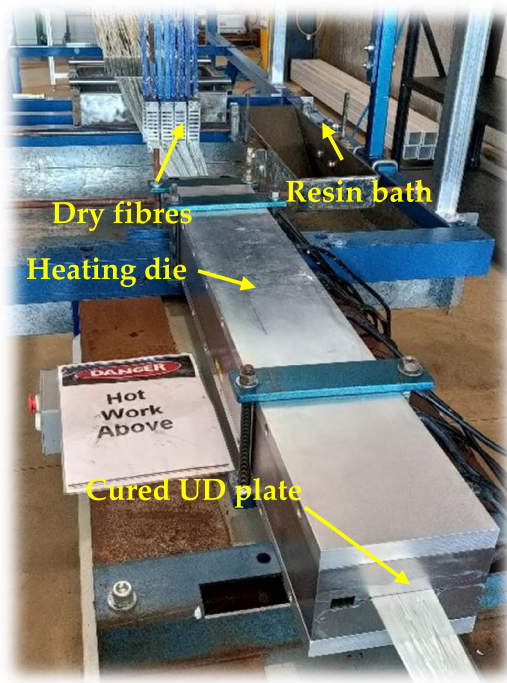
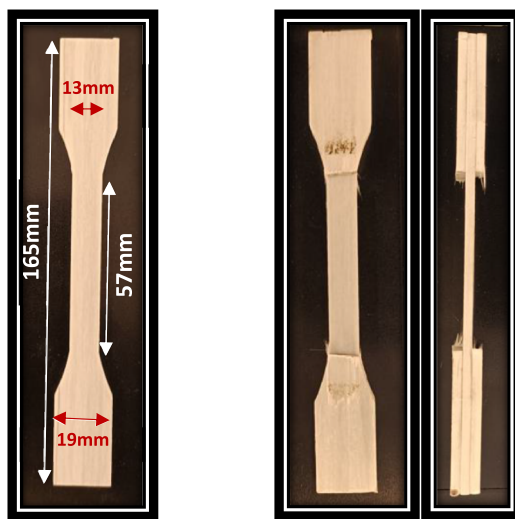


FIGURE 1 Pultrusion process. [Colour figure can be viewed at [wileyonlinelibrary.com](https://onlinelibrary.wiley.com/doi/10.1111/ffe.13979)]



(A) Specimen geometry (B) Typical tapered specimen

FIGURE 2 Specimen details. [Colour figure can be viewed at [wileyonlinelibrary.com](https://onlinelibrary.wiley.com/doi/10.1111/ffe.13979)]

selected to avoid the self-heating effect on the tested samples where the raised temperature during the test should be less than  $8^{\circ}\text{C}$ , as observed by Ferdous et al.<sup>3</sup> and Shah et al.<sup>28</sup> Moreover, as the gripping mechanism was applied by a hydraulic system, the lateral gripping pressure was applied at 7, 10, and 13 MPa to observe the effect of the

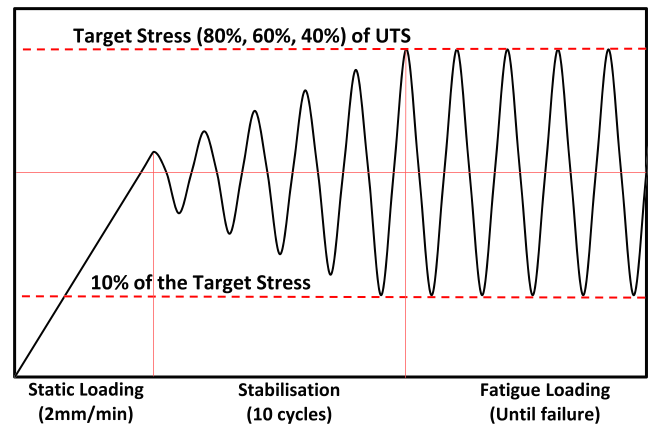


FIGURE 3 Fatigue loading configuration. [Colour figure can be viewed at [wileyonlinelibrary.com](https://onlinelibrary.wiley.com/doi/10.1111/ffe.13979)]

lateral gripping pressure on the fatigue behavior of the FRP composites. Five replicates were tested under quasi-static loading while three replicates for each specimen type were tested to represent each parameter on the stress-number of cycles (S-N) curve.

### 2.3 | Fatigue loading

All tests were carried out under standard laboratory conditions ( $23^{\circ}\text{C} [\pm 1^{\circ}\text{C}]$  and 42%  $[\pm 3\%]$  relative humidity [RH]). Constant amplitude (sinusoidal waveform) fatigue tests were applied on the unidirectional coupon specimens under load control using a 100-kN capacity MTS servo-hydraulic test machine in accordance with ISO 13003.<sup>37</sup> The stress ratio (R) (maximum-to-minimum applied stress wave) was maintained at 10% as recommended by previous works.<sup>2,29,30,38</sup> The typical fatigue loading configuration can be seen in Figure 3. This load scheme was previously adopted by Korhikoski et al.<sup>5</sup> and Ferdous et al.<sup>3</sup>

### 2.4 | Instrumentation and testing machine

MTS machine (Landmark<sup>®</sup> Servo-hydraulic Test Systems-model 370.10) with a 100-kN tension and compression capacity was used to test the specimens. Smooth surface grips were selected to avoid damaging the UD fibers at the tips during the test, which can affect the fatigue behavior of the tested specimens. The load-displacement data were collected by the crosshead load (accuracy of  $\pm 1$  N) and displacement (accuracy of  $\pm 0.01$  mm) acquisition system built within the MTS machine. Previous study (Ferdous et al.<sup>3</sup>) that utilized the



same machine have verified the accuracy of the displacement from the LVDT of the machine using an external LVDT. Moreover, a digital laser thermometer gun (supplied by Smart Sensors) was used to measure the temperature at the surface of the specimens before testing and at failure to determine the temperature difference, which was found to be at  $4^{\circ}\text{C}$  ( $\pm 0.6^{\circ}\text{C}$ ) at 4 Hz and up to  $9^{\circ}\text{C}$  ( $\pm 1.3^{\circ}\text{C}$ ) at 10-Hz frequency (compared to the  $T_g$  of  $138^{\circ}\text{C}$ ).

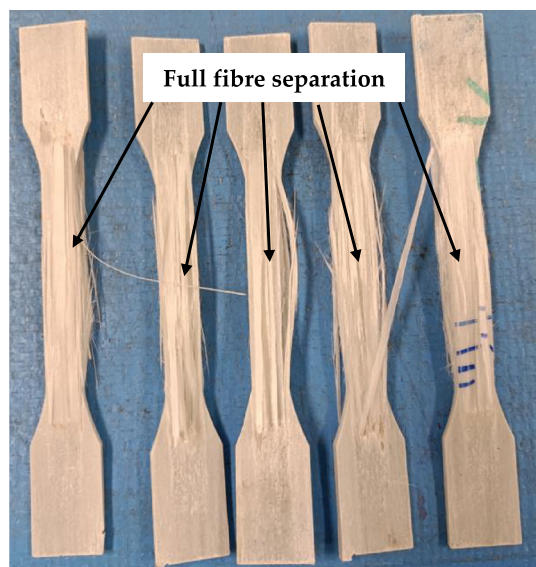


FIGURE 4 Final failure of the quasi-static-tested specimens. [Colour figure can be viewed at [wileyonlinelibrary.com](https://onlinelibrary.wiley.com)]

### 3 | TEST RESULTS AND DISCUSSION

#### 3.1 | Failure mode

Figure 4 shows the failure mode for the control specimens tested under quasi-static loading where a holistic separation in the UD fibers at the testing region can be noticed as expected. On the other hand, testing the specimens under fatigue loading revealed various modes of failure based on the applied stress level and the applied gripping pressure. However, cycles frequency was noticed to affect insignificantly the mode of failure of the tested specimens.

The failure progression of the tested specimens under fatigue started by longitudinal splitting between the UD fibers (debonding) (see Figure 5A,B) and propagated to breakage in these separated fibers, as shown in Figure 5C. Nevertheless, the level of applied stress influenced the severity of the UD fiber debonding. Thus, various modes of failure were noticed in the tested specimens as shown in Figure 6. It can be observed from Figure 7A that specimens tested at 80% stress level showed the closest mode of failure to the ones tested under quasi-static denoted by a full separation between the UD fibers. However, the amount of the separated UD fibers decreased with the decrease in the level of applied stress (see Figure 6A,B). This can be explained by the smaller load distributed along the length of the specimens tested at a lower applied stress, which causes limiting the failure progression to be more localized. This is evidenced by the

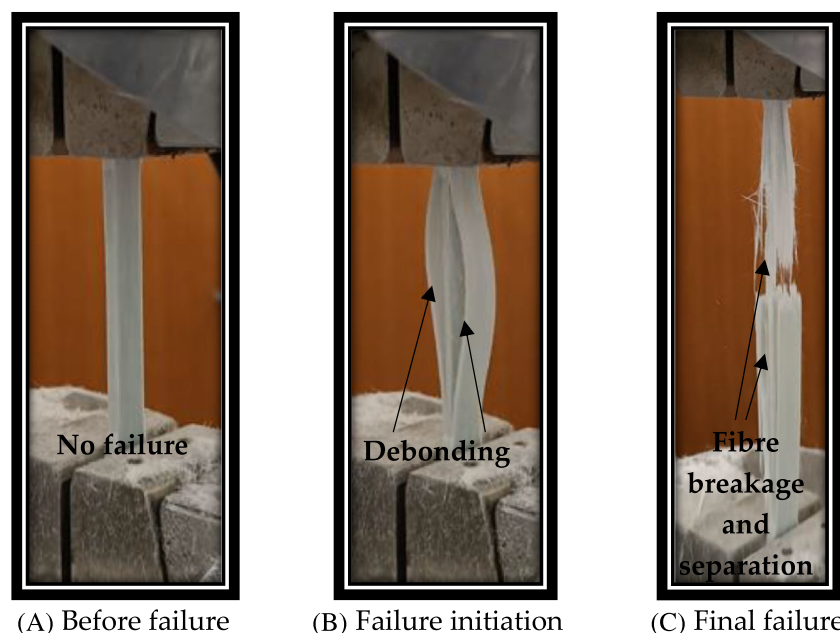


FIGURE 5 Progressive failure of the fatigue-tested specimens. [Colour figure can be viewed at [wileyonlinelibrary.com](https://onlinelibrary.wiley.com)]

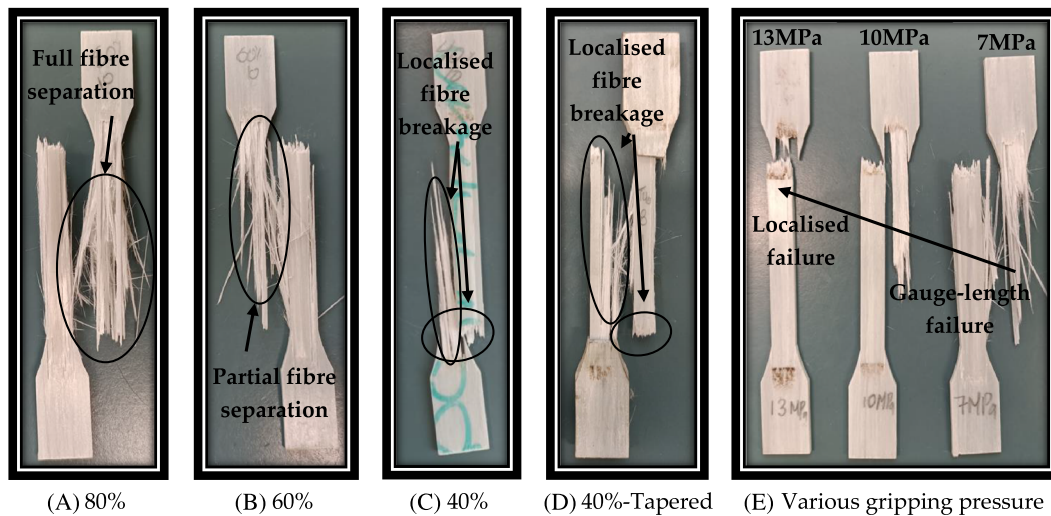


FIGURE 6 Final modes of failure of the tested specimens under fatigue. [Colour figure can be viewed at [wileyonlinelibrary.com](https://onlinelibrary.wiley.com/doi/10.1111/ffe.13979)]

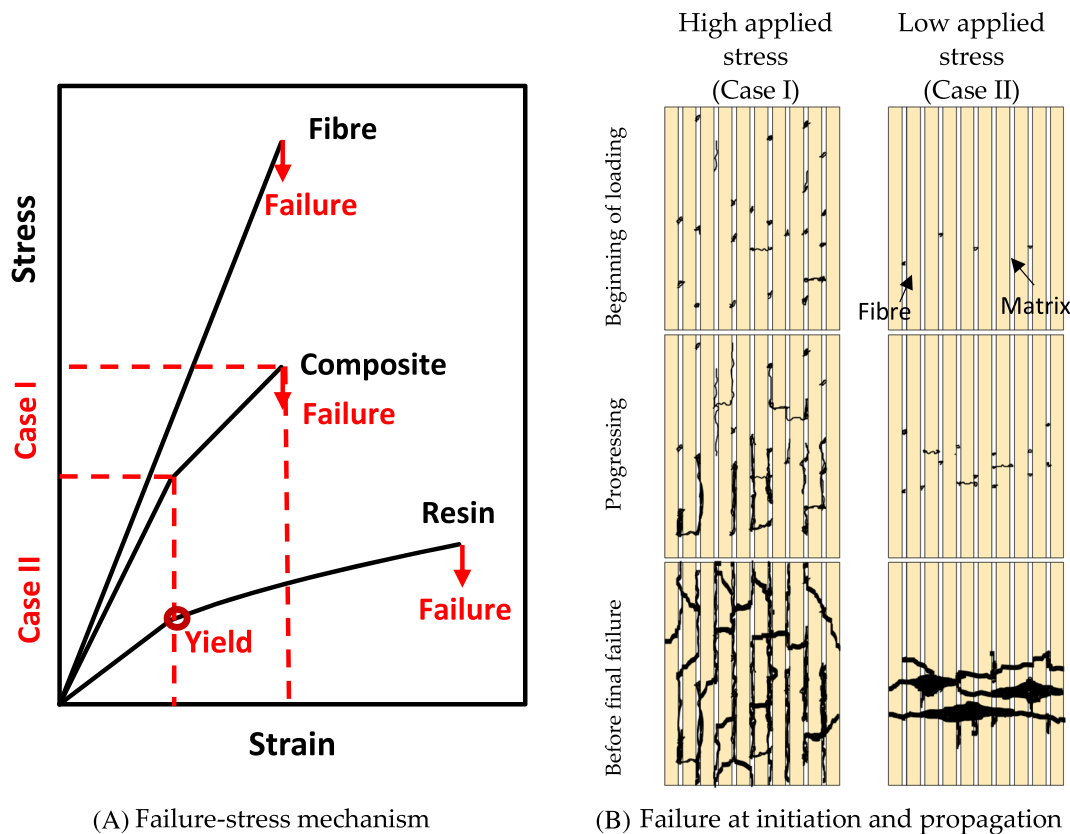


FIGURE 7 Failure mechanism of the tested specimens. [Colour figure can be viewed at [wileyonlinelibrary.com](https://onlinelibrary.wiley.com/doi/10.1111/ffe.13979)]

progressive failure (initiated at several locations) in the specimens tested at high stress level (80%) and those tested at low stress level (40%) in Figure 7A,C, respectively. Furthermore, the tapered specimens at 40% applied stress level showed almost similar failure

behavior to their counterparts tested at 40% stress level without bonded end tabs. However, more localized failure at the ends of the former specimens was observed accompanied by less separation in the UD fibers. This is attributed to the discontinuous stress transfer pathway

from the tab to the testing gauge-length of the specimen as the UD fibers of the specimen and the tab are not connected. This creates a point of stress concentration at which localized failure can be noticed as shown in Figure 6D. Therefore, it is recommended to adopt the dog-bone shape for fatigue testing specimens without end tabs.

Furthermore, the lateral gripping pressure significantly impacted the failure behavior under fatigue of UD composites. Figure 6E shows that the increase in the lateral gripping pressure leads to immature failure at the contact point between the steel grips and the specimen. It is worth highlighting that fiber-reinforced composites are weak in the perpendicular direction to the axis of the fibers. Thus, the increase in the lateral gripping pressure could break the UD fibers even before the start of the test, which results in unrepresentative fatigue life of the UD composites. Thus, this study suggests using low lateral gripping pressure at least to prevent slippage between the specimen and the steel grip, which was 7 MPa in this study.

Figure 7A provides a typical stress-strain behavior of the constituent (fiber and matrix) to better explain the failure mechanism of UD FRP composites under fatigue. According to Figure 7, when the applied fatigue stress is higher than the strength limit for the matrix (the weakest constituent), this leads to initiation of interfacial split/debonding/matrix tear at high applied stress level or lateral-spread micro-cracks at low applied stress. Indeed, in the specimens subjected to high applied stress level (80%), the strength limit of the matrix was approached, which led to highly developed matrix cracking and interfacial debonding between the matrix and fibers causing the separation and damage in

the UD fibers (see Figure 6A and Case I in Figure 7B), whereas the decrease in the applied stress level reduced the matrix cracking to the level of less than the interfacial shear stress between the matrix and fibers. In this case, a phenomenon called fiber-bridge breaking can be noticed (see Figure 6C) where the failure propagates transversely (not along the fibers -see Case II in Figure 7B) to show a local failure in the composite specimen. Due to this, the specimens with end-tabs did not show different mode of failure compared to the ones without.

### 3.2 | Displacement-stress and displacement-time responses

Initially, the tested specimens under static loading recorded an average tensile strength of 1064.8 MPa with standard deviation of 25.7 MPa (Stiffness of 14.6 kN/mm with standard deviation of 0.21 kN/mm). Figure 8 shows the typical displacement-stress and time-displacement behavior of the FRP composites tested at different levels of applied stress. The described mode of failure in the previous section can be reflected in Figure 6. For instance, the specimens tested at 80% stress level showed progressive failure through a gradual degradation in the axial stiffness until the final failure at around 3 mm. By tracking the maximum and minimum displacement in the time-displacement plot in Figure 8A, it can be concluded that specimens at 80% stress level showed failure initiation before reaching half of the fatigue life due to high applied stress level which facilitates faster debonding between the UD fibers. Nevertheless, the gradual increase in the displacement response before reaching

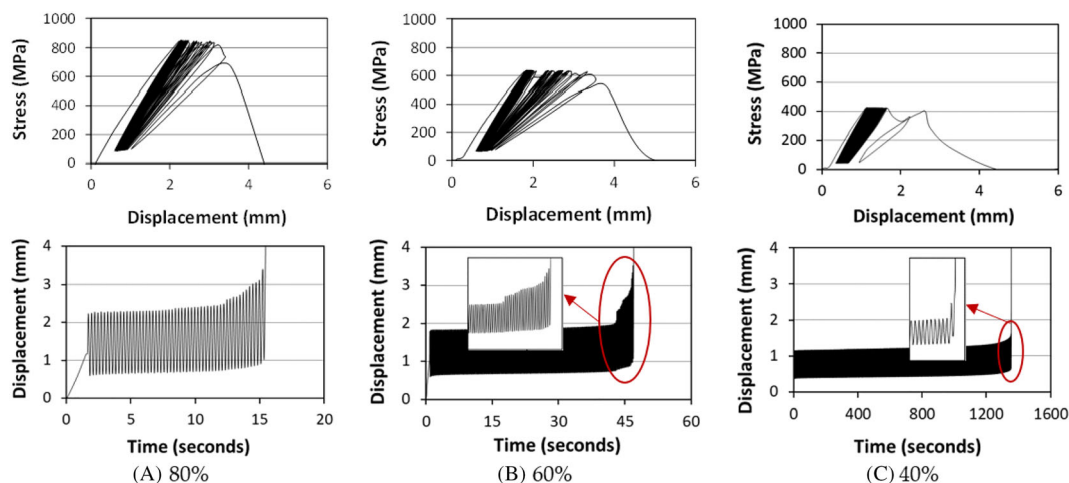


FIGURE 8 Typical stress-displacement and time-displacement behavior of the tested specimens. [Colour figure can be viewed at [wileyonlinelibrary.com](http://wileyonlinelibrary.com)]

the final failure indicates a uniform failure progression leading to a full failure of the gauge-length, as shown in Figure 6A.

Figure 8B showed a uniform displacement-stress response for specimen tested at 60% applied stress level until the failure initiation occurred (i.e., at 2 mm in Figure 8B). This led to a fast decay in the stiffness until the final failure. However, this degradation occurred only in the last 10% of the fatigue life of the tested specimens at 60% stress level as shown by the time-displacement plot even though this 10% time is quite similar to the failure progression time in the specimens tested at 80% stress level. The fatigue resistance in the last 10% of the fatigue lifetime allowed for a reasonable failure progression through distributed separation between the UD fibers before the final failure as shown in Figure 6B with less fiber separation compared to the specimens tested at 80% applied stress level. Figure 8C showed a sudden failure occurred in specimen tested at 40% applied fatigue stress level (i.e., at 1.7 mm in Figure 8C) after a uniform fatigue resistance. It is worth highlighting that when the first debonding occurs (microcracks), the failure propagation depends on the applied stress level where higher applying 80% of ultimate strength resulted in more fiber separation compared to the applied stress level of 60%, as noticed in Figure 8A,B. Thus, the failure of specimens tested at an applied stress level of 40% was localized at the location of the failure initiation (see Figure 6C).

Figure 9 presents the typical axial stiffness of the tested specimens at the first and last fatigue cycles with

respect to different applied stress. It can be noticed that increasing the applied stress level from 40% to 60% and from 40% to 80% reduced the initial stiffness by 4.0% and 9.4%, respectively (see Figure 9A–C). This is due to the early microcracks caused by the high applied level of stress at the beginning. Similar finding was observed by Ferdous et al.<sup>3</sup> and Zangenberg et al.<sup>4</sup> Moreover, gradual stiffness degradation percentage can be observed in Figure 10D with the increase in the applied stress. It should be mentioned that the stiffness was calculated based on the fatigue stiffness of the tested specimens. It is worth mentioning that specimens tested at 80% and 60% stress levels revealed 52.3% and 49.2% stiffness retention before failure. However, the specimens tested at 40% stress level showed only 75.8% stiffness retention before the final failure. It should be mentioned that matrix debonding and interfacial failure leads to a progressive failure, which leads to a higher loss in stiffness, whereas fiber breakage resulted in a brittle and sudden failure without showing progressive stiffness loss before the final failure.<sup>29</sup> This can be evident by the final mode of failure reported in Figure 6A–C.

### 3.3 | Fatigue cycles

Table 1 and Figure 10 report the number of fatigue cycles before failure of UD FRP composites. It can be noticed that the number of cycles significantly increases with the decrease of the applied stress level. However, the

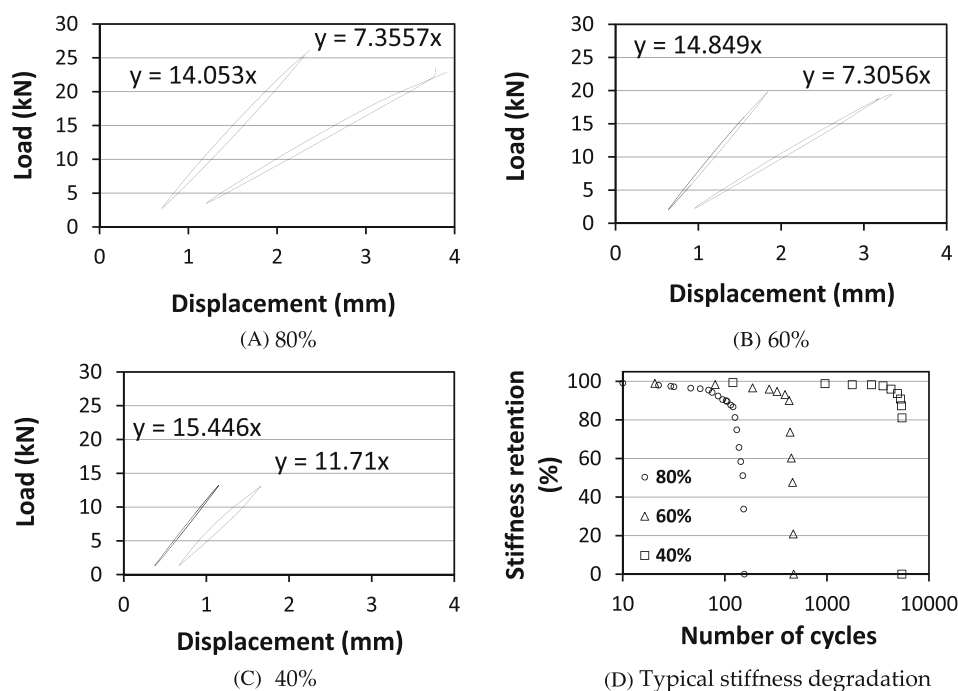
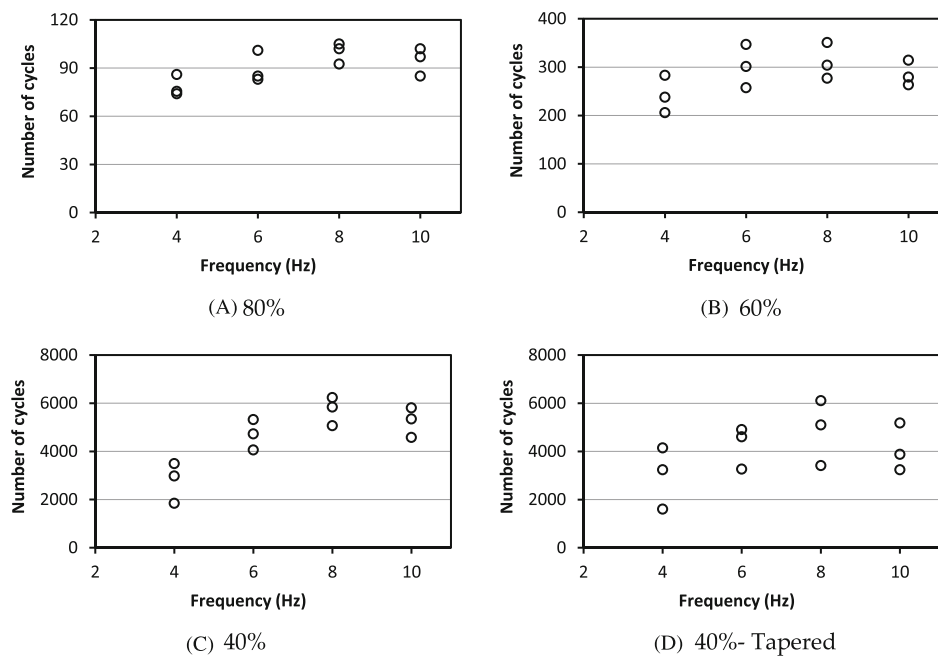


FIGURE 9 Typical stiffness degradation of the tested specimens under various applied stresses.





**FIGURE 10** Effect of applied stress level and frequency on the number of cycles.

decrease rate differs based on the frequency, which becomes more significant with the decrease in the applied stress level. For instance, the decrease in the stress level from 80% to 40% increased the fatigue life by 35 times (78.5 to 2770 cycles) and 55 times (95 to 5243 cycles) for 4 and 10 Hz, respectively. Moreover, it can be observed from Table 1 that the tapered specimens recorded an almost similar number of cycles to the specimens without bonded end tabs. However, a higher standard deviation and coefficient of variation because of the inconsistent mode of failure as described in Section 3.1 (see Figure 6D). Generally, the coefficient of variation increases with the decrease in the applied stress level (see Table 1). This is due to the localized matrix failure and fiber breakage observed in Figure 6C and Figure 7B, which prevents the propagation along the gauge-length of the specimens tested at lower applied stress level (i.e., 40%). This result indicates that the fatigue cycles also depend on the failure initiation location.

The test frequency has no significant influence on the mode of failure, but it has a considerable effect on the fatigue life, especially at lower applied stress level, as can be seen clearly in Table 1 and Figure 10. According to Figure 10, the tested specimens showed an increase in the number of cycles with the increase of the frequency up to 8 Hz, which had the same response as 10 Hz. It should be highlighted that at 40% applied stress level, the specimens recorded a 47% reduction in the number of cycles by comparing the results at 10 Hz and at 4 Hz. Similar findings can be found by Nguyen et al.<sup>39</sup> when they tested unidirectional Vinylester-glass sheets under tension–tension fatigue loading. Nguyen et al.<sup>39</sup> observed

that specimens ( $V_f$  of 30%) tested at 2 Hz recorded fatigue life of almost 20–30% less than the similar specimens tested at 10 Hz. This might be referred to the brief increase in the self-heating at a higher frequency, which leads to make the matrix more elastic and delays the initiation of the cracks as a result.<sup>40</sup>

### 3.4 | Stress-number of cycles (S-N) response

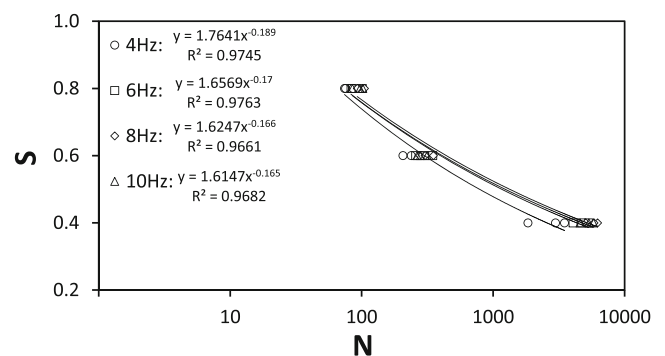
Stress-number of cycles response (as commonly called S-N curve) represents the fatigue life of any material at which empirical formulas can be extracted to predict the fatigue behavior at a certain time. Regarding the tested specimens in this study, it was observed that the maximum number of fatigue cycles reported at 40% stress level ranged from 4000 to 6000 cycles. This number is relatively low compared to other studies on composite materials, which sometimes records millions of cycles.<sup>4,5,17,41</sup> It should be highlighted that the composite manufacturing process and the constituent quantities play a major role in defining the ultimate strength capacity of the composite material. For instance, the increase in the fiber content increases the mechanical properties (strength and stiffness) until however a certain level where these properties will reduce significantly due to insufficient matrix required to bond the filaments together and transfer the internal stresses between them<sup>4,5,25</sup> as well as its brittle nature. Referring to Section 2.1, which showed that the fiber volume fraction of 65%, this percentage is not studied in the literature for the UD glass fiber

**TABLE 1** Fatigue cycles of the tested specimens.

Frequency (Hz)	Applied stress level				
	80%	60%	40%	40%—tapered	
4	74	283	1840	3241	
	75.5	206	2980	4144.5	
	86	238	3491	1604	
	Average	78.5	242.3	2770.3	2996.5
	Standard deviation	5.3	31.6	690.1	1051.5
Coefficient of variation (%)	6.8%	13.0%	24.9%	35.1%	
6	85	347	4723	3264	
	101	301.5	4056	4910	
	83	257.5	5315.5	4608	
	Average	89.7	302.0	4698.2	4260.7
	Standard deviation	8.1	36.5	514.5	715.5
Coefficient of variation (%)	9.0%	12.1%	11.0%	16.8%	
8	102	351	6235	5099	
	105	277	5842	3414	
	92.5	304	5063	6105	
	Average	96.7	310.7	5713.3	4872.7
	Standard deviation	5.3	30.6	487.0	1110.2
Coefficient of variation (%)	5.5%	9.8%	8.5%	22.8%	
10	102	263.5	5346	3241	
	97	279.5	4579	3882	
	85	314.3	5803	5178	
	Average	94.7	285.8	5242.7	4100.3
	Standard deviation	7.1	21.2	505.0	805.7
Coefficient of variation (%)	7.5%	7.4%	9.6%	19.6%	

composite yet as it can be produced by pultrusion or prepreg manufacturing processes. However, the prepreg is a special manufacturing technique mainly for carbon fiber composites due to its relatively high cost. Nevertheless, Sorensen and Goutianos<sup>42</sup> analytically found that the strain fatigue limit decreases significantly with the increase in the fiber volume fraction especially when the  $V_f$  is beyond 60%. This will be explained in detail in the next section. It should be highlighted that the design of high  $V_f$  composites for fatigue applications requires a careful selection of the fiber and resin type to reduce the brittleness of the matrix and increase the bonding between the matrix and resin.

Figure 11 shows the S-N curves of the tested specimens with various frequency values. Considering the power fatigue behavior (based on the Paris fatigue crack growth rate law,<sup>3,16,28</sup> see Equation 1), it can be noticed that the two values control the trend of the S-N curve, that is, the slope factor ( $\alpha$ ) and the power factor ( $\beta$ ). These two factors are influenced by the frequency value.

**FIGURE 11** The S-N curve of the tested specimens.

Thus, Figure 12 shows the relationship between the two factors and the frequency as also reflected in Equations (2) and (3), respectively. In Equation (1), ( $x$ ) represents the number of cycles. It can be noticed that the proposed equations show high correlation coefficient ( $R^2$ )

indicating on the statistical reliability of the test results. It should be mentioned that the proposed equation (1 to 3) is for UD GFRP laminates with 65% fiber volume fraction and using vinyl ester resin, while another proposed simplified model will be presented in the next section accounting for the fiber volume fraction of the composite specimens.

$$S = \alpha \times N^\beta \tag{1}$$

$$\alpha = 1.994 (x)^{-0.1} \tag{2}$$

$$\beta = 0.229 (x)^{-0.15} \tag{3}$$

### 4 | COMPARATIVE ANALYSIS WITH PREVIOUS STUDIES

For quasi-static strength tests, although the increase in the fiber content in composites increases the stiffness and strength, this increase is limited to a certain level where composites start to show a drop in the strength due to an insufficient amount of resin to wet out the surface of the filament properly and transfer the internal stresses effectively.<sup>43</sup> However, the optimal fiber content value is not unified as composites behave orthotopically. In tension-tension fatigue loading of composite having a high fiber volume fraction, similar to this study, the applied stress is observed to significantly affect the fatigue life.<sup>25</sup> This was

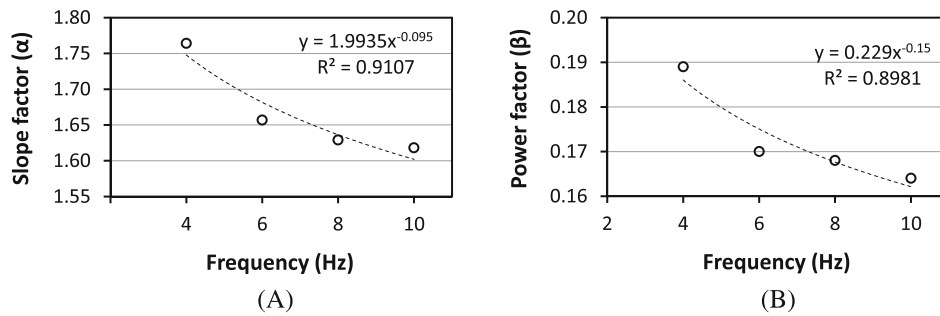
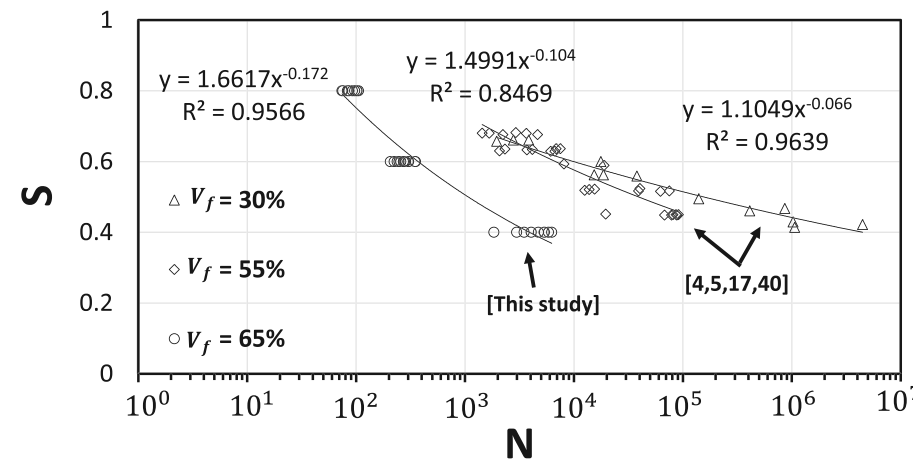


FIGURE 12 The effect of the frequency on the parameters of the S-N curve.



(A) S-N curves of unidirectional glass-reinforced composites with various  $V_f$  ratio

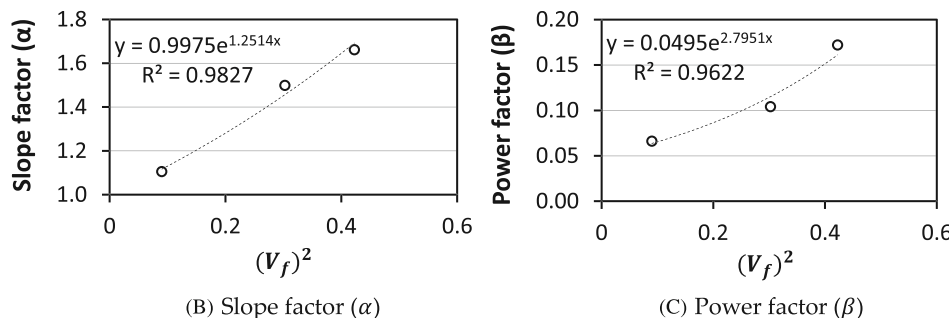


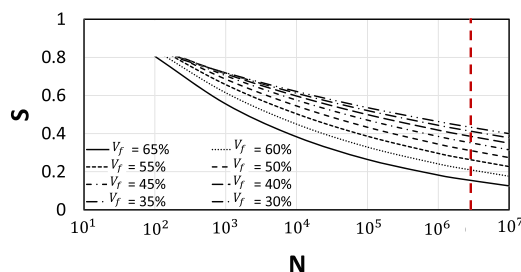
FIGURE 13 S-N behavior of the UD glass FRP composites.

noticed in this study wherein a low fatigue life was measured for UD glass FRP specimens ( $V_f = 65\%$ ) and the change in the mode of failure with various applied stress values (Figure 6). This finding was also observed for carbon fiber and natural fiber composites<sup>28,44</sup> where the reduction in the resin quantity between fibers (especially in the UD composites due to weak transverse mechanical properties) due to the increase in the fiber content makes the fibers very vulnerable to debond owing to the high stress concentration in the interfacial zones. This leads to rapid failure initiation and progression and a reduction in the fatigue life of the composites as a result.

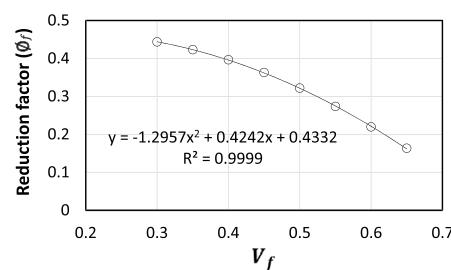
Figure 13 shows the available data of UD glass FRP composites for various fiber volume fraction ( $V_f$ ) subjected to tension–tension fatigue loading from the available literature.<sup>4,5,17,41</sup> While the investigated composites have different fiber content, these studies were considered because of their close stress amplitude adopted during testing, similar resin type (thermoset resin), and fiber alignment (longitudinal) to the loading. Figure 13A shows the significant negative influence of  $V_f$  on the fatigue life of the UD glass FRP composites. In the contrary, the quasi-static strength capacity is higher for the specimens with higher  $V_f$ . This can be explained by the different mechanisms of both tests in which the quasi-static tension test shows a fiber-based property where the load is mainly carried by the fibers. In contrast, the repetitive load mode engages the resin to transfer the fluctuating stresses through the cross-section (between fibers), which results in a high stress concentration zone due to its weaker mechanical properties compared to the fibers. This results in lower cycle fatigue life of unidirectional composites with high fiber content as the resin quantity will be small and not sufficient to handle high applied stress as a proportion of the maximum quasi-static strength. This issue can be overcome by using off-axis fibers, which can release the stress concentration on the resin prolonging the cyclic fatigue life of composites.

In Figure 13B,C, the slope factor ( $\alpha$  in Equation 2) and power factor ( $\beta$  in Equation 3) were found to have strong relationship with  $V_f$  (Equations 4 and 5, respectively). Thus, based on the available data, the fatigue life of the UD glass FRP composites can be given by Equation (1) where  $\alpha$  and  $\beta$  are given in Equations (4) and (5), respectively. It should be noted that additional tests can be attempted to consider various resin and fiber types, fiber orientation, and stress ratio.

A reduction factor for design purposes of the UD glass FRP composites under fatigue loading is proposed based on the results of this study and from comparable studies gathered from available literature. Equations (1), (4), and (5) were used to generate the S-N curves of UD glass FRP composite with different  $V_f$ , as shown in Figure 14A. Afterwards, the attained stress in the S-N curves (in Figure 14A) to reach 2 million cycles (as adopted by<sup>18,23,45</sup>) was selected to be a reduction factor given in Equation (6). For fatigue life design purposes of UD composites, it can be indicated that a reduction factor of 0.16, 0.32, and 0.40 can be suggested for composites with  $V_f$  of 65%, 50%, and 40%, respectively. This might be also applied to the reinforcing GFRP rods with UD fiber alignment. Noël and Soudki<sup>46</sup> tested GFRP bars with 12 mm in diameter ( $V_f$  around 55%) under 40% and 29% tension–tension fatigue loading with a frequency of 4 Hz. They found that the failure occurred at 95,000 cycles only in the specimens tested at 40% applied stress, whereas specimens tested under 29% applied stress achieved the 2 million cycles as a fatigue life. According to Equation (6), interestingly, the reduction factor on the applied stress level at  $V_f$  of 55% is 27.5%, which is very close to the applied stress level of 29% in the Noël and Soudki<sup>46</sup> study. This indicates the significance of adopting the proposed reduction factor on the applied stress level to achieve the target fatigue life of UD composites.



(A) Applied stress vs number of cycles



(B) Reduction factor value vs fibre volume fraction

FIGURE 14 The proposed fatigue reduction factor of UD glass FRP composites. [Colour figure can be viewed at [wileyonlinelibrary.com](https://onlinelibrary.wiley.com)]



$$\alpha = (e)^{1.25(V_f)^2} \quad (4)$$

$$\beta = 0.05 (e)^{2.80(V_f)^2} \quad (5)$$

$$\emptyset_f = 0.43 + 0.42V_f - 1.3V_f^2 \quad (6)$$

## 5 | CONCLUSIONS

This study investigated the fatigue behavior (mode of failure, number of cycles, and stiffness reduction) of pultruded UD glass FRP (GFRP)-vinyl ester composites with fiber volume fraction ( $V_f$ ) of 65% under different test parameters including applied stress level (80%, 60%, and 40%), frequency (4, 6, 8, and 10 Hz), and end conditions (with and without tabs). The influence of the frequency on the tested specimens was analyzed. Moreover, a simplified model was proposed to describe the fatigue life of the UD glass FRP composites considering the volume fiber fraction. The following conclusions are drawn from this study:

- Decreasing the applied stress level (e.g., from 80% to 40%) increased the fatigue cycles at failure and changed the failure mode of UD GFRP composites from fibers separation to local fiber breakage caused by local stress concentration.
- UD glass FRP composites will exhibit a more stable and longer fatigue life at 8 and 10 Hz than at 4 and 6 Hz. This could refer to the brief increase in the self-heating, which softens the vinyl ester resin delaying the crack initiation and progression.
- The dog-bone shape specimens gave a more reliable fatigue performance for UD GFRP composites compared to those with end tabs. Moreover, the lateral gripping pressure significantly affected the fatigue behavior of the UD FRP glass composites due to end crushing because of the low transverse stiffness of the glass fibers.
- The fiber volume fraction significantly affected the fatigue life of the UD glass FRP composites where composites with higher volume fraction will exhibit lower fatigue resistance than the composites with lower fiber volume.
- A reduction factor based on the value of  $V_f$  is proposed to maximize the performance of UD GFRP composites and to assist designers in the design to consider their long-term fatigue capacity. UD GFRP composites with 40% fibers can be designed up to 40% of their stress limits up to 2 million fatigue cycles but should be

limited to only 16% of their stress limits when the fiber volume fraction is at 65%.

- From the engineering and applicability point of view, this study recommends using the high fiber volume fraction GFRP composites for static applications as they have high stiffness and strength, whereas low fiber volume fraction GFRP composites are recommended for fatigue applications.

It can be recommended that further manufacturing trials of unidirectional FRP composites with different levels of  $V_f$  using the same manufacturing process can be conducted to validate and refine the proposed fatigue reduction factor. This will ensure the reliability of the developed model and eliminate discrepancy in the process history. Investigating the fatigue behavior of FRP composites with different types of fibers and resin as well as fiber geometries including off-axis fiber layers will assist in increasing confidence and use of these advanced materials in various engineering applications.

### AUTHOR CONTRIBUTIONS

**Omar Alajarmeh:** Conceptualization; resources; testing; visualization; writing—original draft. **Allan Manalo, Wahid Ferdous, Ghassan Almasabha, Ahmad Tarawneh, Khaled Eayal Awwad, Alexander Safonov:** Analysis; writing—review and editing. **Xuesen Zeng and Peter Schubel:** Project administration; resources; supervision; management.


### ACKNOWLEDGMENTS

The authors would like to acknowledge the assistance of the technician at the Centre for Future Materials-University of Southern Queensland. The authors acknowledge the financial support of the Advance Queensland Industry Research Fellowship Program (AQIRF128-2021). Open access publishing facilitated by University of Southern Queensland, as part of the Wiley - University of Southern Queensland agreement via the Council of Australian University Librarians.

### DATA AVAILABILITY STATEMENT

The data that support the findings of this study are available from the corresponding author upon reasonable request.

### ORCID

**Omar Alajarmeh**  <https://orcid.org/0000-0002-9446-5436>

**Ghassan Almasabha**  <https://orcid.org/0000-0002-1414-3913>

**Ahmad Tarawneh**  <https://orcid.org/0000-0002-9945-7582>

## REFERENCES

- Manalo A, Aravinthan T, Fam A, Benmokrane B. State-of-the-art review on FRP sandwich systems for lightweight civil infrastructure. *J Compos Constr.* 2017;21(1):04016068.
- Hashin Z, Rotem A. A fatigue failure criterion for fiber reinforced materials. *J Compos Mater.* 1973;7(4):448-464.
- Ferdous W, Manalo A, Peauril J, et al. Testing and modelling the fatigue behavior of GFRP composites—effect of stress level, stress concentration and frequency. *Eng Sci Technol Int J.* 2020; 23(5):1223-1232.
- Zangenberg J, Brøndsted P, Gillespie JW Jr. Fatigue damage propagation in unidirectional glass fibre reinforced composites made of a non-crimp fabric. *J Compos Mater.* 2014;48(22):2711-2727.
- Korkiakoski S, Brøndsted P, Sarlin E, Saarela O. Influence of specimen type and reinforcement on measured tension–tension fatigue life of unidirectional GFRP laminates. *Int J Fatigue.* 2016;85:114-129.
- Mandell JF, Samborsky DD. DOE/MSU composite material fatigue database: test methods, materials, and analysis, Sandia National Lab. (SNL-NM), Albuquerque, NM (United States). 1997.
- Kawai M. A phenomenological model for off-axis fatigue behavior of unidirectional polymer matrix composites under different stress ratios. *Compos a: Appl Sci Manuf.* 2004;35(7–8): 955-963.
- Mohammadi B, Fazlali B. Off-axis fatigue behavior of unidirectional laminates based on a microscale fatigue damage model under different stress ratios. *Int J Fatigue.* 2018;106:11-23.
- Maji A, Acree R, Satpathi D, Donnelly K. Evaluation of pultruded FRP composites for structural applications. *J Mater Civil Eng.* 1997;9(3):154-158.
- Alajarmeh O, Zeng X, Aravinthan T, et al. Compressive behaviour of hollow box pultruded FRP columns with continuous-wound fibres. *Thin-Walled Struct.* 2021;168:108300.
- Yuksel O, Sandberg M, Hattel JH, Akkerman R, Baran I. Mesoscale process modeling of a thick pultruded composite with variability in fiber volume fraction. *Materials.* 2021;14(13):3763.
- Alhawamdeh M, Alajarmeh O, Aravinthan T, et al. Modelling hollow pultruded FRP profiles under axial compression: local buckling and progressive failure. *Compos Struct.* 2021;262: 113650.
- Alhawamdeh M, Alajarmeh O, Aravinthan T, et al. Modelling flexural performance of hollow pultruded FRP profiles. *Compos Struct.* 2021;276:114553.
- Alhawamdeh M, Alajarmeh O, Aravinthan T, et al. Review on local buckling of hollow box FRP profiles in civil structural applications. *Polymers.* 2021;13(23):4159.
- Jessen S, Plumtree A. Fatigue damage accumulation in pultruded glass/polyester rods. *Composites.* 1989;20(6):559-567.
- Allah MHA, Abdin EM, Selmy A, Khashaba U. Effect of fibre volume fraction on the fatigue behaviour of GRP pultruded rod composites. *Compos Sci Technol.* 1996;56(1):23-29.
- Samborsky DD. Fatigue of E-glass fiber reinforced composite materials and substructures, Citeseer. 1999.
- Brunbauer J, Stadler H, Pinter G. Mechanical properties, fatigue damage and microstructure of carbon/epoxy laminates depending on fibre volume content. *Int J Fatigue.* 2015;70: 85-92.
- Pan N. Theoretical determination of the optimal fiber volume fraction and fiber-matrix property compatibility of short fiber composites. *Polym Compos.* 1993;14(2):85-93.
- Shah DU, Schubel PJ, Licence P, Clifford MJ. Determining the minimum, critical and maximum fibre content for twisted yarn reinforced plant fibre composites. *Compos Sci Technol.* 2012; 72(15):1909-1917.
- Roe P, Ansell MP. Jute-reinforced polyester composites. *J Mater Sci.* 1985;20(11):4015-4020.
- Demers C. Tension–tension axial fatigue of E-glass fiber-reinforced polymeric composites: tensile fatigue modulus. *Construct Build Mater.* 1998;12(1):51-58.
- Wu Z, Wang X, Iwashita K, Sasaki T, Hamaguchi Y. Tensile fatigue behaviour of FRP and hybrid FRP sheets. *Compos Part B Eng.* 2010;41(5):396-402.
- Ferdous W, Manalo A, Yu P, et al. Tensile fatigue behavior of polyester and vinyl ester based GFRP laminates—a comparative evaluation. *Polymers.* 2021;13(3):386.
- Mini K, Lakshmanan M, Mathew L, Mukundan M. Effect of fibre volume fraction on fatigue behaviour of glass fibre reinforced composite. *Fatigue Fract Eng Mater Struct.* 2012;35(12): 1160-1166.
- Sevenois R, Van Paepegem W. Fatigue damage modeling techniques for textile composites: review and comparison with unidirectional composite modeling techniques. *Appl Mech Rev.* 2015;67(2):020802.
- Brunbauer J, Pinter G. Effects of mean stress and fibre volume content on the fatigue-induced damage mechanisms in CFRP. *Int J Fatigue.* 2015;75:28-38.
- Shah DU, Schubel PJ, Clifford MJ, Licence P. Fatigue life evaluation of aligned plant fibre composites through S–N curves and constant-life diagrams. *Compos Sci Technol.* 2013;74: 139-149.
- Zhao X, Wang X, Wu Z, Keller T, Vassilopoulos AP. Effect of stress ratios on tension–tension fatigue behavior and micro-damage evolution of basalt fiber-reinforced epoxy polymer composites. *J Mater Sci.* 2018;53(13):9545-9556.
- Toth I. *Creep and Fatigue Behavior of Unidirectional and Crossplied Composites.* ASTM International; 1969.
- Khan R, Alderliesten R, Badshah S, Benedictus R. Effect of stress ratio or mean stress on fatigue delamination growth in composites: critical review. *Compos Struct.* 2015;124: 214-227.
- ASTM E1269. *Standard Test Method for Determining Specific Heat Capacity by Differential Scanning Calorimetry.* Conshohocken, PA: ASTM West; 2011.
- ASTM D3171. *Standard Test Methods for Constituent Content of Composite Materials.* Conshohocken, PA: ASTM West; 2015.
- ASTM D3479. *Standard Test Method for Tension-Tension Fatigue of Polymer Matrix Composite Materials.* ASTM International; 2012.
- ASTM D638. *Standard Test Method for Tensile Properties of Plastics.* ASTM international; 2014.
- ASTM D3039. *Standard Test Method for Tensile Properties of Polymer Matrix Composite Materials.* ASTM international; 2014.
- ISO-13003. *Fibre-reinforced Plastics—Determination of Fatigue Properties Under Cyclic Loading Conditions.* International Organization for Standardization; 2003.

38. Vieira PR, Carvalho EML, Vieira JD, Toledo Filho RD. Experimental fatigue behavior of pultruded glass fibre reinforced polymer composite materials. *Compos Part B Eng*. 2018;146:69-75.
39. Tinh Nguyen HT, Chuang T-j, Chin J, Wu F, Lesko J. *A Fatigue Model for Fiber-reinforced Polymeric Composites for Offshore Applications*. Washington, USA: Virginia Polytechnic Institute and State University; 2000.
40. AlAjarmeh O, Manalo A, Benmokrane B, et al. Compression behavior of GFRP bars under elevated in-service temperatures. *Construct Build Mater*. 2022;314:125675.
41. Mandell J, Samborsky D, Scott M. *DOE-MSU Wind Turbine Blade Composite Material Fatigue Database*. Montana, USA: Department of Chemical Engineering, Montana State University at Boznan; 2003.
42. Sørensen BF, Goutianos S. *Prediction of Fatigue Limit for Unidirectional Carbon Fibre/Epoxy Composites*. IOP Conference Series: Materials Science and Engineering. Vol. 388. IOP Publishing; 2018:012017.
43. Kollar LP, Springer GS. *Mechanics of Composite Structures*. Cambridge University Press; 2003.
44. Kim H, See S, Pitkethly M, Bader M, Deguchi T, Kim H, Ikeda T. Prediction of fatigue limit for unidirectional carbon fibre/epoxy composites.
45. Wu C, Feng P, Bai Y. Comparative study on static and fatigue performances of pultruded GFRP joints using ordinary and blind bolts. *J Compos Constr*. 2015;19(4):04014065.
46. Noël M, Soudki K. Fatigue behavior of GFRP reinforcing bars in air and in concrete. *J Compos Constr*. 2014;18(5):04014006.

**How to cite this article:** AlAjarmeh O, Manalo A, Ferdous W, et al. Fatigue behavior of unidirectional fiber-reinforced pultruded composites with high volume fiber fraction. *Fatigue Fract Eng Mater Struct*. 2023;46(6):2034-2048. doi:[10.1111/ffe.13979](https://doi.org/10.1111/ffe.13979)